HHS Public Access
Author manuscript
Inorg Chem. Author manuscript; available in PMC 2022 March 28.

Published in final edited form as:
Inorg Chem. 2022 January 10; 61(1): 37–41. doi:10.1021/acs.inorgchem.1c03468.

Nonheme Diiron Oxygenase Mimic That Generates a Diferric–Peroxo Intermediate Capable of Catalytic Olefin Epoxidation and Alkane Hydroxylation Including Cyclohexane

Williamson N. Oloo,
Department of Chemistry, University of Minnesota, Minneapolis, Minnesota 55455, United States

Miklós Szávuly,
Research Group of Bioorganic and Biocoordination Chemistry, University of Pannonia, 8200 Veszprém, Hungary

József Kaizer,
Research Group of Bioorganic and Biocoordination Chemistry, University of Pannonia, 8200 Veszprém, Hungary

Lawrence Que Jr.
Department of Chemistry, University of Minnesota, Minneapolis, Minnesota 55455, United States

Abstract

Herein are described substrate oxidations with H_2O_2 catalyzed by $[Fe^{II}(IndH)(CH_3CN)_3](ClO_4)_2$ [IndH = 1,3-bis(2′-pyridylimino)isoindoline], involving a spectroscopically characterized (*μ*-oxo)(*μ*-1,2-peroxo)diiron(III) intermediate (2) that is capable of olefin epoxidation and alkane hydroxylation including cyclohexane. Species 2 also converts ketones to lactones with a decay rate dependent on [ketone], suggesting direct nucleophilic attack of the substrate carbonyl group by the peroxo species. In contrast, peroxo decay is unaffected by the addition of olefins or alkanes, but the label from $H_2{}^{18}O$ is incorporated into the the epoxide and alcohol products, implicating a high-valent iron–oxo oxidant that derives from O–O bond cleavage of the peroxo intermediate. These results demonstrate an ambiphilic diferric–peroxo intermediate that mimics the range of oxidative reactivities associated with O_2-activating nonheme diiron enzymes.

Nonheme diiron enzymes are involved in many oxidative metabolic pathways.[1] This class includes those that hydroxylate strong C–H bonds like soluble methane monooxygenase (sMMO)[2] and deoxyhypusine hydroxylase (hDOHH), which helps to regulate cell proliferation in humans.[3] These enzymes activate O_2 at diiron(II) active sites that form (*μ*-1,2-peroxo)diiron(III) centers called **P**.[4a,5] For sMMO, **P** converts into a diiron(IV)

Corresponding Authors: **József Kaizer** – *Research Group of Bioorganic and Biocoordination Chemistry, University of Pannonia, 8200 Veszprém, Hungary*; kaizer@almos.uni-pannon.hu; **Lawrence Que, Jr.** – *Department of Chemistry, University of Minnesota, Minneapolis, Minnesota 55455, United States*; larryque@umn.edu.

Supporting Information
The Supporting Information is available free of charge at https://pubs.acs.org/doi/10.1021/acs.inorgchem.1c03468.
Additional data and experimental details (PDF)

Complete contact information is available at: https://pubs.acs.org/10.1021/acs.inorgchem.1c03468

The authors declare no competing financial interest.

intermediate **Q** that is directly responsible for methane oxidation.[4b] An analogous O–O bond cleavage step is proposed for hDOHH,[5b] but the putative high-valent oxidant has not been trapped. Yet another diiron enzyme, cyanobacterial aldehyde deformylating oxygenase (cADO), converts fatty aldehydes into alkanes, a reaction initiated by nucleophilic attack of the corresponding peroxo intermediate on the aldehyde functionality of the substrate.[6,7] These examples illustrate the mechanistic diversity of the peroxodiiron(III) unit in this family of enzymes.

In recent years, synthetic peroxodiiron(III) complexes have served to model such nonheme diiron enzyme intermediates.[1] Kodera et al. have described a (μ-oxo)(μ-1,2-peroxo)diiron-(III) complex supported by a bis-TPA [TPA = tris(pyridyl-2-methyl)amine] ligand that undergoes O–O bond cleavage to oxidize the benzylic C–H bonds of toluene.[8] More recently, Kaizer et al. have reported a peroxodiferric species supported by 2-(4-thiazolyl)benzimidazole ligands that exhibits ambiphilic reactivity in aldehyde deformylation, oxidation of the O–H bonds of phenols, and oxidative demethylation of DMA.[9] In this study, we focus on another (μ-oxo)(μ-1,2-peroxo)diiron(III) intermediate that exhibits even greater oxidative versatility.

Previously, $[Fe^{II}(IndH)(CH_3CN)_3](ClO_4)_2$ [**1**; IndH = 1,3-bis(2′-pyridylimino)isoindoline] has been found to react with H_2O_2 at 25 °C in acetonitrile (MeCN) to form a transient green species **2** (Figure 1 left). This species has been identified as $[Fe^{III}_2(\mu\text{-O})(\mu\text{-1,2-O}_2)(IndH)_2(solv)_2]^{2+}$ and shown to oxidize thioanisoles and benzyl alcohols.[10a] Remarkably, we herein demonstrate **2** to be an even more versatile and powerful oxidant that converts cyclic ketones to lactones, epoxidizes olefins, and even oxidizes cyclohexane.

In a previous publication, we reported that **2** decayed over 10 min at 5 °C with k_{decay} = $1.16(5) \times 10^{-3}$ s^{-1} (Figure S1) and with $\Delta H^{\ddagger}$ = 81(5) kJ mol^{-1} and $\Delta S^{\ddagger}$ = −10(10) J mol^{-1} K^{-1} (Figure S2a), reflecting a unimolecular decay process.[10a,b] In our current study, we find that the addition of cyclohexanone accelerates its decay at rates that depend linearly on [cyclohexanone] (Figure 1, left), indicating a direct reaction between **2** and cyclohexanone with k_2 = 0.4 M^{-1} s^{-1}. Caprolactone is formed with up to 12.5 TON (relative to **1**; see Table 1), demonstrating catalytic conversion of cyclohexanone to caprolactone. Under these conditions, the decay of **2** exhibits $\Delta H^{\ddagger}$ = 22(1) kJ mol^{-1} and $\Delta S^{\ddagger}$ = −170(10) J mol^{-1} K^{-1} (Figure S2a), parameters similar to those for PhCHO oxidation by **2**.[10b] When the experiment is carried out in the presence of $H_2{}^{18}O$, no ^{18}O is incorporated into the lactone product (Figure S2b), analogous to Baeyer–Villiger oxidations.[11] Complex **2** thus acts as a nucleophilic oxidant (Scheme 1, top left) and represents a rare example of a diferric–peroxo complex that performs the role proposed for the corresponding intermediate in the cADO mechanism.[7]

More significant than acting as a nucleophilic oxidant, **2** also carries out catalytic electrophilic hydrocarbon oxidation (Table 1). Unlike its reaction with cyclohexanone, **2** decays at a rate of ~0.02 s^{-1} at 25 °C, which is independent of the nature of the hydrocarbon and its concentration (Figure S3). These results show that **2** itself cannot be the actual oxidant but must evolve into a more powerful species to generate the oxidized products (Figure 1, right). Interestingly, the second-order rate constants associated with hydrocarbon oxidation show a linear dependence on [substrate] (Figure 2, left) and span over a 1000-fold range, with O-atom transfer to a C═C bond being much faster than C–H bond cleavage (Table 1). These observations indicate that the rate-determining step for these catalytic reactions must involve substrate oxidation. Kinetic measurements of toluene oxidation (see the Table S2 data with the gray background and Figure S4) show a first-order (not half-order) dependence on [**2**], excluding the possibility that **2** dissociates into two mononuclear Fe^{IV}═O units.

The oxidative reactivity of **2** resembles that of nonheme Fe^{IV}═O complexes.[12] As shown in Figure 2 (right), there is a linear correlation between the logarithms of the product formation rate constants normalized per equivalent target H atom for substrates that undergo C–H bond attack versus C–H bond dissociation enthalpies (BDEs), showing that C–H bond cleavage is an important component of the product formation step. In addition, a nonclassical H/D kinetic isotope effect (KIE) of 37 for toluene is observed (Figure S4), concurring with Kodera's observations for a related diiron catalyst supported by a dinucleating ligand.[8b] Such large nonclassical values are associated with nonheme iron(IV) oxo complexes[12] and are much larger than the classical values for catalytic alkane hydroxylations by mononuclear Fe(L)/H_2O_2 systems involving Fe^{V}═O oxidants.[13]

Further insight into the nature of the oxidant has been obtained from $H_2{}^{18}O$-labeling experiments, which show significant label incorporation into the oxidized products. As much as 40–50% ^{18}O is incorporated into the PhS(O)Me, cyclooctene oxide, and Ph_3COH products, which represent three different types of reactions (Table 1). Because labeled oxygen from $H_2{}^{18}O$ cannot exchange into a peroxide moiety without prior O–O bond cleavage, the results show that the actual oxidant in these electrophilic reactions must involve a species formed subsequent to O–O bond cleavage of **2** and capable of undergoing label exchange with $H_2{}^{18}O$. When examined as a function of the $H_2{}^{18}O$ concentration, the % ^{18}O incorporated into cyclooctene oxide increases linearly with [$H_2{}^{18}O$] but plateaus above 0.6 M $H_2{}^{18}O$ (Figure 3, left). This saturation behavior implicates a reversible H_2O binding step prior to O-atom transfer to the substrate. Indeed, the high degree of ^{18}O-label incorporation observed indicates reaction conditions that approach complete equilibration within the putative $Fe^{IV}(O)(OH_2)$ unit. Moreover, ^{18}O-label incorporation into cyclooctene oxide is found to be independent of the cyclooctene concentration (10–300 equiv; Figure S6), suggesting that ^{18}O-label exchange is much more facile than substrate oxidation.

The observed saturation behavior for ^{18}O incorporation in cyclooctene oxidation (Figure 3, left) resembles that reported for Fe(TPA)-catalyzed hydrocarbon oxidations with H_2O_2 as the oxidant.[14] For the latter, the percentage of incorporation of ^{18}O from $H_2{}^{18}O$ into cyclohexanol and cyclooctane-1,2-diol products increased linearly with [$H_2{}^{18}O$] and maximized above 0.3 M with added H_2O. These results were rationalized by $H_2{}^{18}O$ exchange into the site *cis* to the hydroperoxo unit on the $[(TPA)Fe^{III}(OOH)(solv)]^{2+}$ intermediate. Subsequent O–O bond heterolysis formed a putative *cis*-$Fe^{V}(O)(^{18}OH)$ oxidant, which, in turn, underwent oxo–hydroxo tautomerization to introduce ^{18}O to the high-valent Fe═O unit, thereby accounting for the observed partial ^{18}O labeling of the products. An analogous mechanism can be formulated for **2**, which has an available site on each Fe center for label exchange with $H_2{}^{18}O$ to allow ^{18}O incorporation into the putative high-valent $O{=}Fe^{IV}{-}O{-}Fe^{IV}{=}O$ oxidant **3** (Scheme 1). Oxidant **3** is analogous to the oxidant that Kodera postulated for his diferric–peroxo intermediate, which is supported by an octadentate 6,6′-(ethylene-bridged)-bis(TPA) ligand,[8] but the Kodera oxidant does not have solvent-exchangeable sites that allow exchange with $H_2{}^{18}O$ to afford the labeled products.

This proposed mechanism is further supported by the drop in % ^{18}O incorporation found for the cyclooctene oxide product with increasing equivalents of pyridine-*N*-oxide (PyO) added into the reaction mixture, reflecting the competition between PyO and H_2O for the labile sixth site on each Fe (Figure 3, right). Furthermore, introducing 1 equiv of the more basic 4-MeO-PyO instead of PyO results in a lower % ^{18}O incorporation, while adding 1 equiv of the less basic 4-NO_2-PyO has very little effect. These results show that PyO competes with $H_2{}^{18}O$ for binding to **2** in Scheme 1. As a control, PyO added to the reaction mixture in place of H_2O_2 produces no epoxide, showing that PyO does not act as an oxidant in this reaction.

Given that **2** can carry out both nucleophilic and electrophilic transformations, we have also conducted competitive oxidations between cyclohexanone and 1-octene or toluene. Consistent with our mechanistic hypothesis, electrophilic oxidation products decrease in yield with higher [cyclohexanone], raising the yield of caprolactone (Figure 4). These results show that nucleophilic oxidation of cyclohexanone competes with the O–O bond cleavage step required to generate the electrophilic oxidant responsible for 1-octene or toluene oxidation.

Among the many diferric–peroxo complexes characterized thus far as models for peroxo intermediates in nonheme diiron enzymes,[1] **2** stands out as the only synthetic diferric–peroxo species reported to date found to oxidize cyclohexane and the only one that carries out both nucleophilic *and* electrophilic oxidations under catalytic conditions. Specifically, **2** catalytically converts cyclohexanone to caprolactone in competition with the epoxidation of C═C bonds and the hydroxylation of aliphatic C–H bonds as strong as those in cyclohexane (Table 1). In fact, caprolactone formation is favored over epoxidation and hydroxylation (Figure 4). Whereas the rate of **2** decay is dependent on the cyclohexanone concentration, it is unaffected by the addition of either olefins or alkanes. These results show that **2** reacts directly with cyclohexanone to initiate its lactonization but must evolve into a more powerful oxidant that oxidizes the latter substrates. In support, ^{18}O from $H_2{}^{18}O$ is incorporated into the epoxide and alcohol products (Table 1), indicating prior cleavage of the O–O bond of *2* to form the high-valent iron–oxo species that oxidizes the hydrocarbons. Diferric–peroxo intermediate **2** is thus quite a versatile reagent, with its diverse reactivity supporting the notion that nonheme diiron enzymes share a common diferric–peroxo intermediate that can be tuned to perform the electrophilic functions of hydroxylases like sMMO and the nucleophilic functions of deformylating enzymes like cADO.[1]

Supplementary Material

Refer to Web version on PubMed Central for supplementary material.

ACKNOWLEDGMENTS

This work is dedicated to the memory of Professor Elena Rybak-Akimova, an enthusiastic investigator of iron–oxygen chemistry. This work was supported by the Hungarian Research Fund (Grants K108489, TKP2020-IKA-07, and GINOP-2.3.2-15-2016-00049 to J.K.) and the U.S. National Institutes of Health (Grants R01 GM-38767 and R35 GM-131721 to L.Q.).

REFERENCES

(1). Jasniewski AJ; Que L Jr. Dioxygen Activation by Nonheme Diiron Enzymes: Diverse Dioxygen Adducts, High-Valent Intermediates, and Related Model Complexes. Chem. Rev 2018, 118, 2554–2592. [PubMed: 29400961]

(2). Banerjee R; Jones JC; Lipscomb JD Soluble Methane Monooxygenase. Annu. Rev. Biochem 2019, 88, 409–431. [PubMed: 30633550]

(3). Wolff EC; Kang KR; Kim YS; Park MH Posttranslational Synthesis of Hypusine: Evolutionary Progresion and Specificity of the Hypusine Modifocation. Amino Acids 2007, 33, 341–350. [PubMed: 17476569]

(4). (a)Liu KE; Valentine AM; Wang D; Huynh BH; Edmondson DE; Salifoglou A; Lippard SJ Characterization of a Diiron(III)-Peroxo Intermediate in the Reaction Cycle of Methane Monooxygenase Hydroxylase from *Methylococcus capsulatus* (Bath). J. Am. Chem. Soc 1995, 117, 10174–10185.(b)Lee S-K; Fox BG; Froland WA; Lipscomb JD; Münck E A Transient Intermediate of the Methane Monooxygenase Catalytic Cycle Containing an $Fe^{IV}Fe^{IV}$ Cluster. J. Am. Chem. Soc 1993, 115, 6450–6451.

(5). (a)Vu VV; Emerson JP; Martinho M; Kim YS; Münck E; Park MH; Que L Jr. Human Deoxyhypusine Hydroxylase, an Enzyme Involved in Regulating Cell Growth, Activates O_2 with a Nonheme Diiron Center. Proc. Natl. Acad. Sci. U. S. A 2009, 106, 14814–14819. [PubMed: 19706422] (b)Jasniewski AJ; Engstrom LM; Vu VV; Park MH; Que L X-ray Absorption Spectroscopic Characterization of the Diferric-peroxo Intermediate of Human Deoxyhypusine Hydroxylase in the Presence of its Substrate eIF5a. JBIC, J. Biol. Inorg. Chem 2016, 21, 605–618. [PubMed: 27380180]

(6). Schirmer A; Rude MA; Li X; Popova E; del Cardayre SB Microbial Biosynthesis of Alkanes. Science 2010, 329, 559–562. [PubMed: 20671186]

(7). Pandelia ME; Li N; Nørgaard H; Warui DM; Rajakovich LJ; Chang W.-c.; Booker SJ; Krebs C; Bollinger JM Jr. Substrate-Triggered Addition of Dioxygen to the Diferrous Cofactor of Aldehyde-Deformylating Oxygenase to Form a Diferric-peroxo Intermediate. J. Am. Chem. Soc 2013, 135, 15801–15812. [PubMed: 23987523]

(8). (a)Kodera M; Kawahara Y; Hitomi Y; Nomura T; Ogura T; Kobayashi Y Reversible O-O Bond Scission of Peroxo-diiron(III) to High-spin Oxodiiron(IV) in Oxygen Activation of a Diiron Center with a Bistpa Dinucleating Ligand as a Soluble Methane Monoxygenase Model. J. Am. Chem. Soc 2012, 134, 13236–13239. [PubMed: 22839735] (b)Kodera M; Ishiga S; Tsuji T; Sakurai K; Hitomi Y; Shiota Y; Sajith PK; Yoshizawa K; Mieda K; Ogura T Formation and High Reactivity of the *anti*-Dioxo Form of High-Spin *μ*-Oxodioxodiiron(IV) as the Active Species That Cleaves Strong C–H Bonds. Chem. - Eur. J 2016, 22, 5924–5936. [PubMed: 26970337] (c)Kodera M; Itoh M; Kano K; Funabiki T; Reglier M A Diiron Center Stabilized by a Bis-TPA Ligand as a Model of Soluble Methane Monooxygenase: Predominant Alkene Epoxidation with H_2O_2. Angew. Chem., Int. Ed 2005, 44, 7104–7106.

(9). Török P; Unjaroen D; Viktória Csendes F; Giorgi M; Browne WR; Kaizer J A Nonheme Peroxodiiron(III) Complex Exhibiting Both Nucleophilic and Electrophilic Oxidation of Organic Substrates. Dalton Trans. 2021, 50, 7181–7185. [PubMed: 34019062]

(10). (a)Pap JS; Cranswick MA; Balogh-Hergovich É; Baráth G; Giorgi M; Rohde GT; Kaizer J; Speier G; Que L An Iron(II)[1,3-bis(2′-pyridylimino)isoindoline] Complex As a Catalyst for Substrate Oxidation with H_2O_2: Evidence for a Transient Peroxodiiron(III) Species. Eur. J. Inorg. Chem 2013, 2013, 3858–3866. [PubMed: 24587695] (b)Kripli B; Szávuly M; Csendes FV; Kaizer J Functional Models of Nonheme Diiron Enzymes: Reactivity of the *μ*-Oxo-*μ*-1,2-peroxo-diiron(III) Intermediate in Electrophilic and Nucleophilic Reactions. Dalton Trans. 2020, 49, 1742–1746. [PubMed: 31967142]

(11). (a)Cho J; Jeon S; Wilson SA; Liu LV; Kang EA; Braymer JJ; Lim MH; Hedman B; Hodgson KO; Valentine JS; Solomon EI; Nam W Structure and Reactivity of a Mononuclear Non-haem Iron(III)-Peroxo Complex. Nature 2011, 478, 502–505. [PubMed: 22031443] (b)McDonald AR; Van Heuvelen KM; Guo Y; Li F; Bominaar EL; Münck E; Que L Jr. Characterization of a Thiolate Iron(III) Peroxy Dianion Complex. Angew. Chem., Int. Ed 2012, 51, 9132–9136. (c)Shokri A; Que L Jr. Conversion of Aldehyde to Alkane by a Peroxoiron(III) Complex, A Functional Model for the Cyanobacterial Aldehyde Deformylating Oxygenase. J. Am. Chem. Soc 2015, 137, 7686–7691. [PubMed: 26030345]

(12). (a)Kaizer J; Klinker EJ; Oh NY; Rohde J-U; Song WJ; Stubna A; Kim J; Münck E; Nam W; Que L Jr. Nonheme $Fe^{IV}O$ Complexes That Can Oxidize the C–H Bonds of Cyclohexane at Room Temperature. J. Am. Chem. Soc 2004, 126, 472–473. [PubMed: 14719937] (b)Biswas AN; Puri M; Meier KK; Oloo WN; Rohde GT; Bominaar EL; Münck E; Que L Jr. Modeling TauD-*J*: A High-Spin Nonheme Oxoiron(IV) Complex with High Reactivity Towards C–H Bonds. J. Am. Chem. Soc 2015, 137, 2428–2431. [PubMed: 25674662] (c)Mitra M; Nimir H; Demeshko S; Bhat SS; Malinkin SO; Haukka M; Lloret-Fillol J; Lisensky GC; Meyer F; Shteinman AA; Browne WR; Hrovat DA; Richmond MG; Costas M; Nordlander E Nonheme Iron(IV)-Oxo Complexes of Two New Pentadentate Ligands and Their Hydrogen-Atom and Oxygen-Atom Transfer Reactions. Inorg. Chem 2015, 54, 7152–7164. [PubMed: 26198840] (d)Monte Pérez I; Engelmann X; Lee Y-M; Yoo M; Kumaran E; Farquhar ER; Bill E; England J; Nam W; Swart M; Ray K A Highly Reactive Oxoiron(IV) Complex Supported by a Bioinspired N3O Macrocyclic Ligand. Angew. Chem., Int. Ed 2017, 56, 14384–14388.

(13). (a)Chen K; Que L Jr. Stereospecific Alkane Hydroxylation by Nonheme Iron Catalysts: Mechanistic Evidence for an $Fe^{V}{=}O$ Active Species. J. Am. Chem. Soc 2001, 123, 6327–6337. [PubMed: 11427057] (b)Chen K; Costas M; Kim J; Tipton AK; Que L Jr. Olefin *cis*-Dihydroxylation versus Epoxidation by Nonheme Iron Catalysts: Two Faces of an Fe^{III}–OOH Coin. J. Am. Chem. Soc 2002, 124, 3026–3035. [PubMed: 11902894]

(14). (a)Bernadou J; Meunier B ‘Oxo-hydroxo Tautomerism’ as a Useful Mechanistic Tool in Oxygenation Reactions Catalysed by Water-soluble Metalloporphyrins. Chem. Commun 1998, 2167–2173.(b)Puri M; Company A; Sabenya G; Costas M; Que L Jr. Oxygen-Atom Exchange Between H_2O and Nonheme Oxoiron(IV) Complexes: Ligand Dependence and Mechanism. Inorg. Chem 2016, 55, 5818–5827. [PubMed: 27275633]

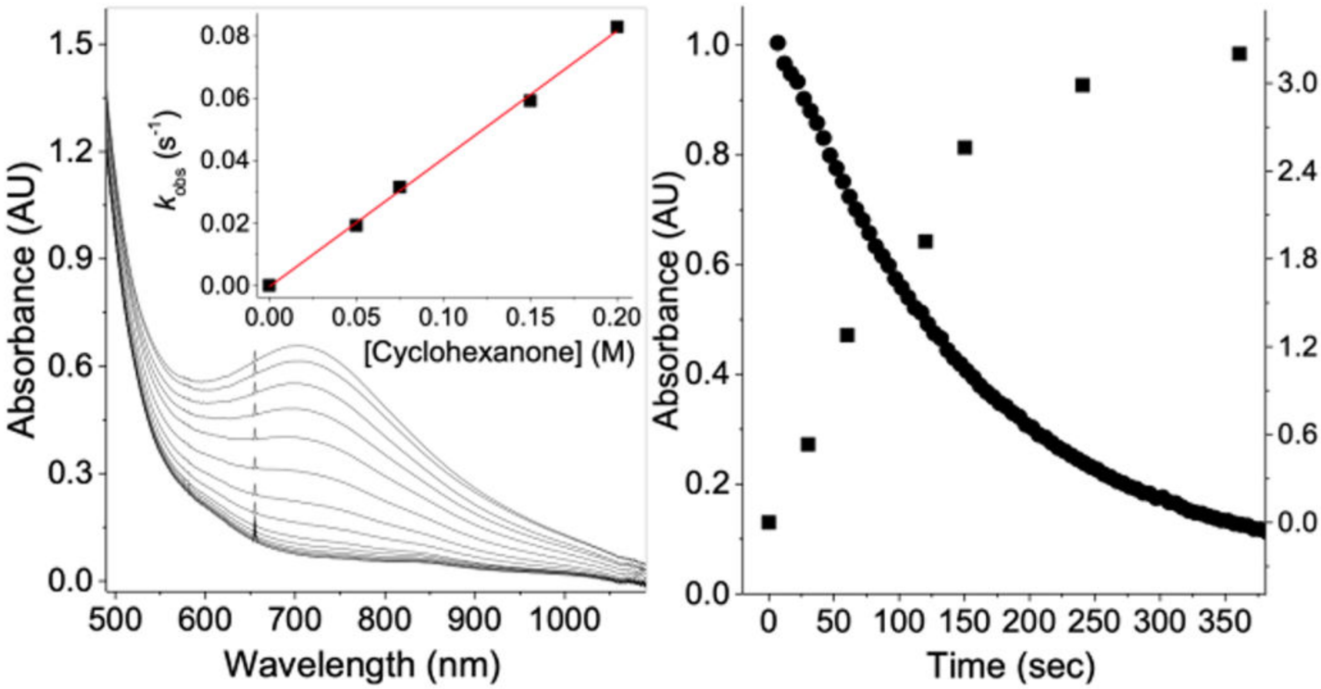

Figure 1.

Left: Spectral changes upon cyclohexanone oxidation by **2** in MeCN at 5 °C with [**1**] = 0.5 × 10^{-3} M and [H_2O_2] = 2.0 mM. Inset: Plot of the rate constants for **2** decay versus [cyclohexanone]. Right: Oxidation of cyclohexane (0.1 M) by **1** (1 mM) and H_2O_2 (0.1 M) at 25 °C, monitoring the change in [**2**] (●) at 680 nm and the concentration of cyclohexanone formed (mM, ■) versus time.

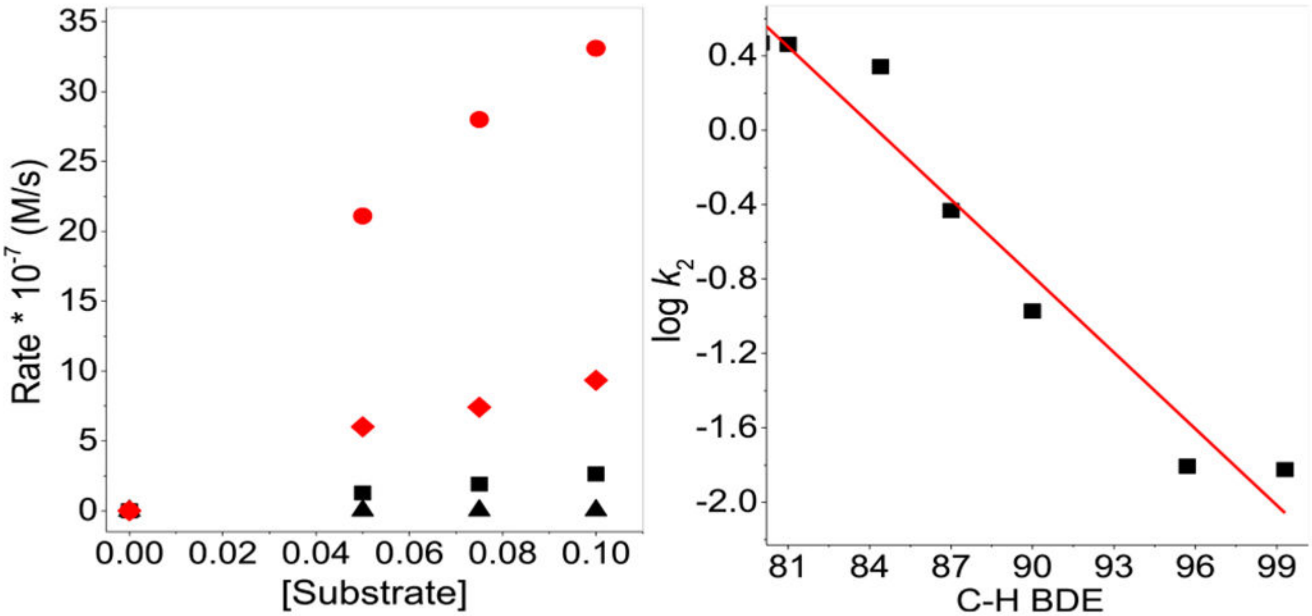

Figure 2.

Left: Plot of the product formation rates versus [substrate] in reactions of cyclooctene (red ●), 1-octene (red ◆), cumene (black ■), and cyclohexane (black ▲) with 0.05 mM **1** and 250 mM H_2O_2 in CH_3CN at 25 °C. Right: Linear correlation between log k_{ox} per substrate H atom and the corresponding C–H BDEs.

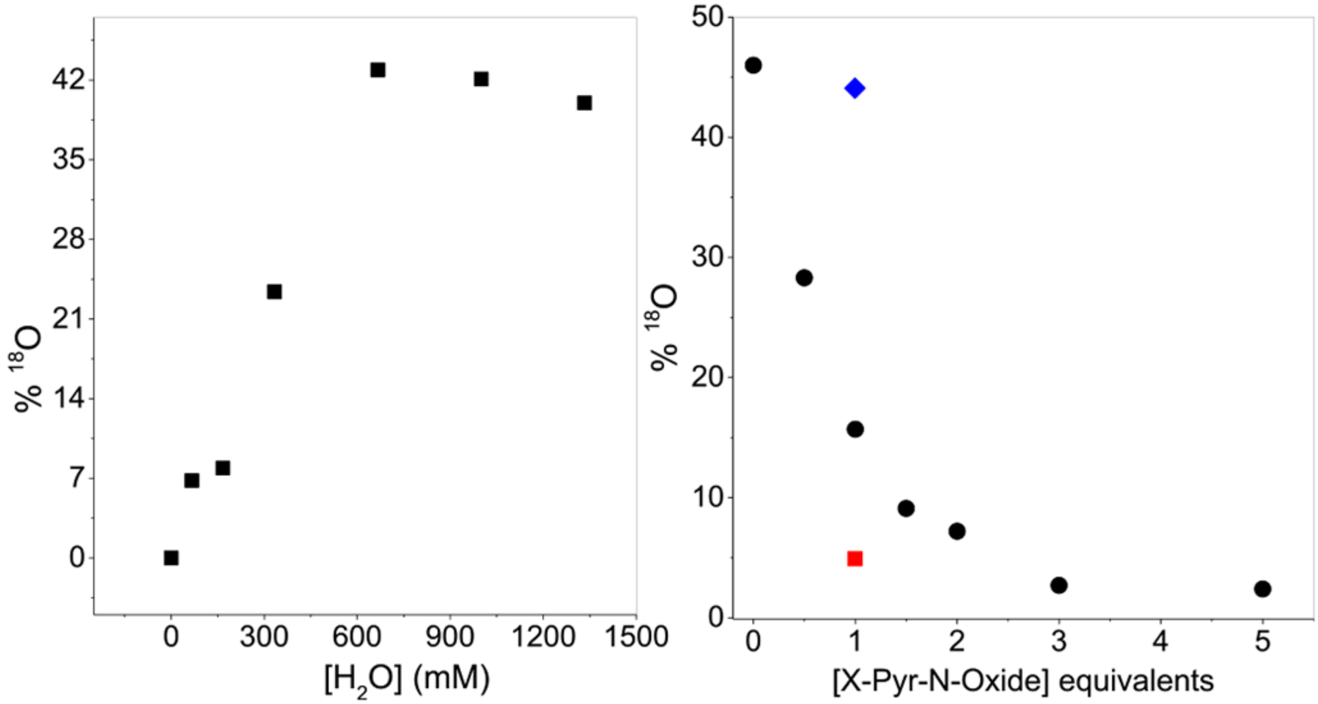

Figure 3.
Left: Plot of % ^{18}O incorporation into product versus [$H_2{}^{18}O$] in cyclooctene oxidation (300 equiv) with **1** and H_2O_2 (5 equiv) in CH_3CN at 25 °C. Right: % ^{18}O labeling of the epoxide product of cyclooctene (200 equiv) by **1** (4 mM), H_2O_2 (2 equiv), and $H_2{}^{18}O$ (250 equiv), with added PyO (black ●), 4-MeO-PyO (red ■), or 4-NO_2-PyO (blue ◆).

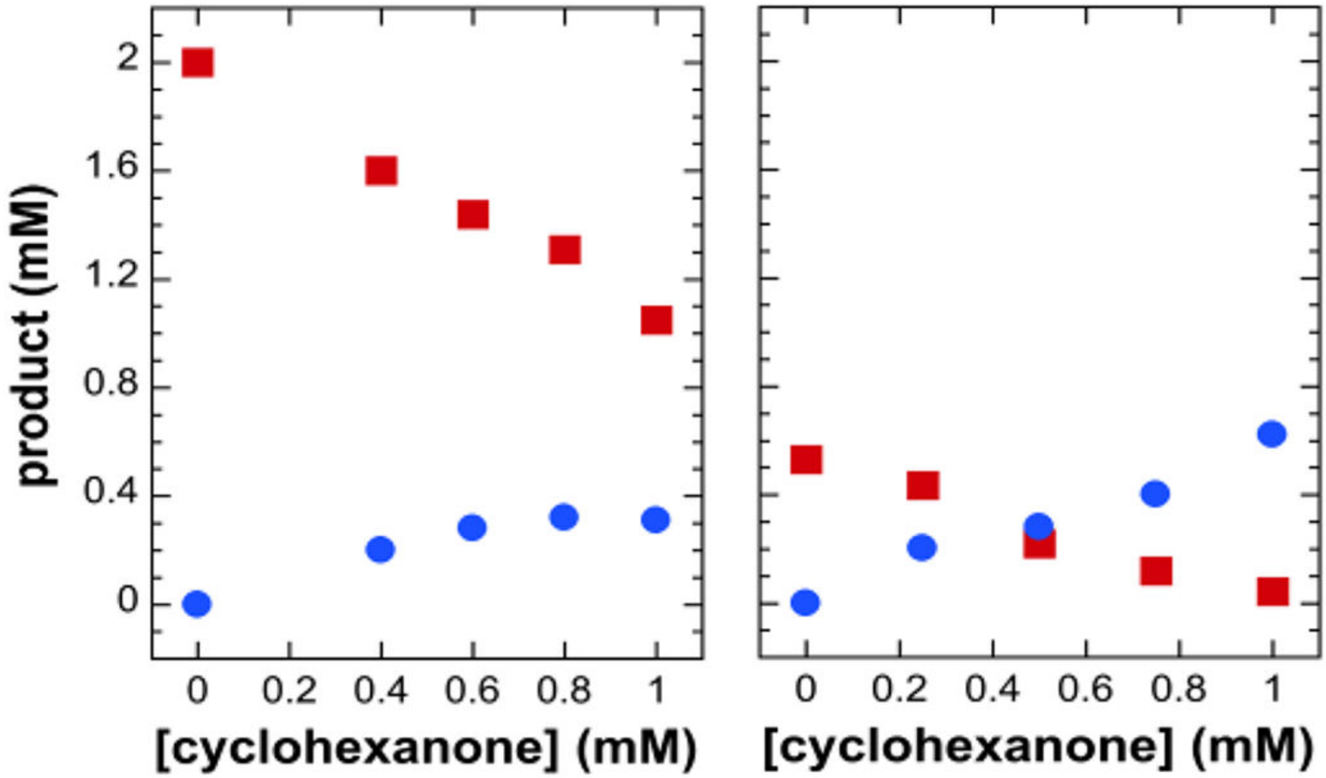

Figure 4.

Yields of 1-octene oxide (red ■, left) and PhCHO (red ■, right) from the oxidations of 1-octene (left) and toluene (right) by **1**/H_2O_2 versus added cyclohexanone. Caprolactone, the cyclohexanone oxidation product, is represented by blue ● in both panels. Reaction conditions: 0.1 mM **1**, 0.25 M H_2O_2, 0.1 M substrate in CH_3CN, 25 °C.

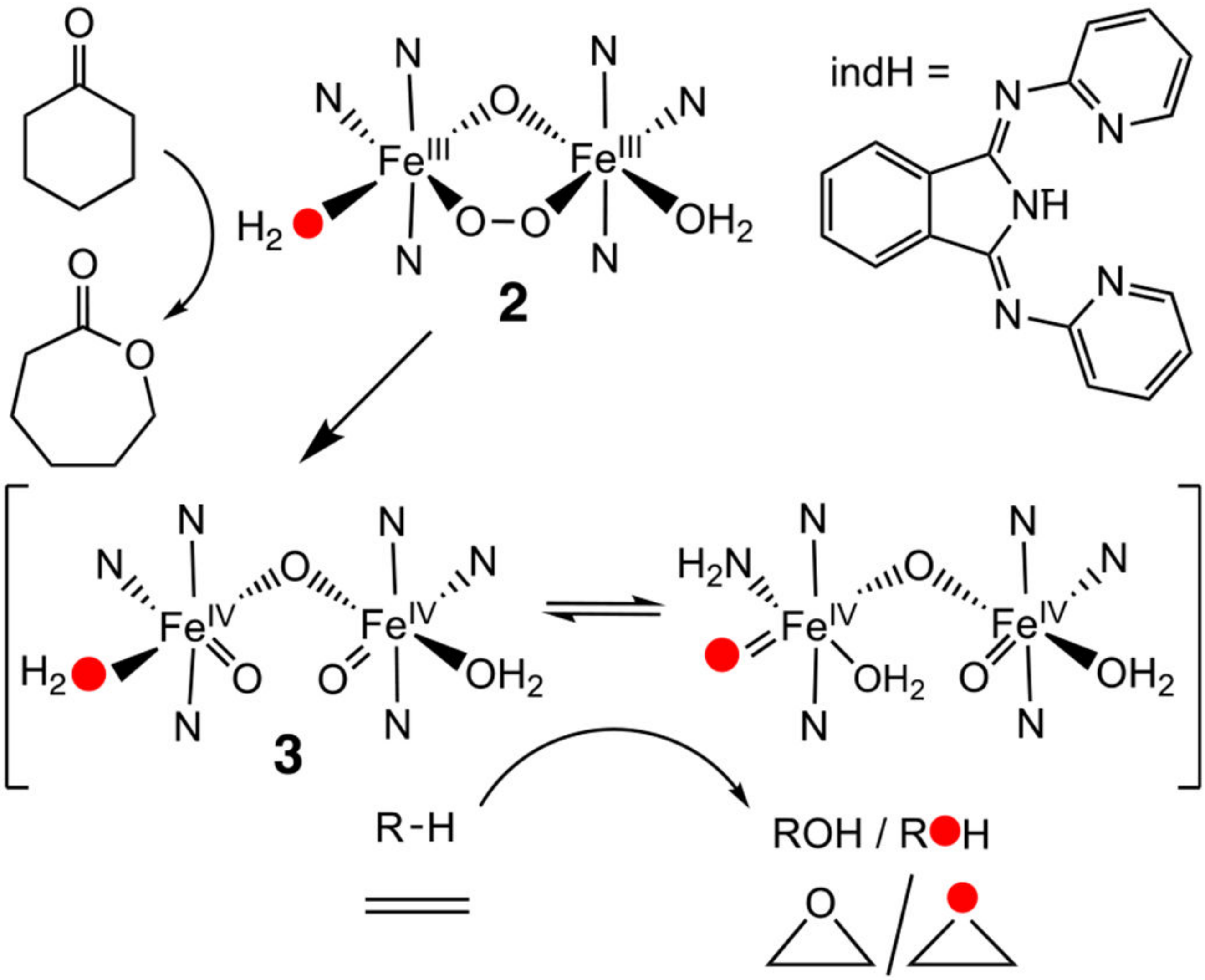

Scheme 1.
Proposed Oxidation Mechanism via 2

Table 1.

Substrate Oxidation Rates at 25 °C, Products, and Turnover Numbers for 1-Catalyzed Reactions[a]

substrate [D_{C-H} in kcal mol^{-1}]	k_2 (M^{-1} s^{-1})	product [% ^{18}O][b]	TON
cyclohexanone	0.4	caprolactone	13
PhSMe	10.5	PhS(O)Me [43][b]	56
cyclooctene	4.2	epoxide [44][b]	36
1-octene	1.2	epoxide	20
Ph_3CH [81]	0.072	Ph_3COH [50][b]	10
$PhCH(CH_3)_2$ [84]	0.054	cumyl alcohol	7
$PhCH_2CH_3$ [87]	0.019	PhC(O)Me	12
$PhCH_3$ [90]	0.008	PhCHO (KIE 37; Hammett $H_\rho = -0.42$)	5
c-C_8H_{16} [96]	0.0062	$C_8H_{14}O$	7
c-C_6H_{12} [99]	0.0045	$C_6H_{10}O$	3

[a]0.1 mmol of substrate, 0.25 mmol of H_2O_2, 1 μmol of **1**, and 10 mL of CH_3CN.

[b]% ^{18}O label incorporated into oxidation products. Reaction conditions: 4 mM **1**, 4 mM H_2O_2, 250 mM substrate, 25 °C.